Chemical Papers (2024) 78:1635–1646
https://doi.org/10.1007/s11696-023-03191-7

ORIGINAL PAPER

Robust superhydrophobic resin sponges modified by polydimethylsiloxanes/epoxy-based copolymer for high-efficiency oil/water separation

Tongyao Zhang[1] · Litao Ma[1] · Dazhong Ren[2] · Ying Huang[1] · Hanpeng Zhang[1]

Received: 21 July 2023 / Accepted: 30 October 2023 / Published online: 19 November 2023

Abstract
The development of recyclable, durable and widely adaptable porous hydrophobic materials is of vital importance for the effective separation of leaking oil–water mixtures. Herein, we functionally modified melamine formaldehyde resin sponge (MFRS) with PMMA, PDMS-PMMA and PDMS-PGMA via a facile solution-immersion process. Compared with PMMA-coated MFRS, the improvement of the water contact angle (WCA) and oil–water mixture separation efficiency of PDMS-PMMA/MFRS was sufficient enough to verify that the introduction of PDMS block enhanced the hydrophobic performances. Moreover, the importance of the GMA block in PDMS-PGMA/MFRS was confirmed by the excellent performance of the material in oil–water separation recycling experiments, with 91.5% separation efficiency after 8 runs. The fabricated PDMS-PMMA/MFRS with improved WCA (155°) and oil–water mixture separation efficiency (99.1%) demonstrated superhydrophobic property, which was attributed to the introduction of hydrophobic block PDMS and coating-induced surface geometric folds. Besides, the acid resistance and widely adaptable (efficient separation of various oil–water mixtures) performances of PDMS-PGMA/MFRS were experimentally confirmed. The freely available manufacturing raw materials and facile functionalization process of PDMS-PMMA/MFRS offer possibilities for its adoption in the efficient cleanup of oil spills.

Keywords Oil–water separation · Copolymer · Superhydrophobic coating · Solution-immersion process · Reusability

Introduction

Oil is the most important energy source and raw material for human production, and it includes different types such as, petroleum, animal fat and vegetable oil (Gryznova et al. 2019; Amina et al. 2022). However, leak cases of during oil transportation have caused serious environmental pollution in recent years (Zhang et al. 2013). Oil floating on water surfaces restricts the flow of oxygen into water columns, which in turn threatens the survival of aquatic organisms. More seriously, fish and fishery products may be exposed to poisoning by the intermediate products of oil degradation, and they become harmful to humans when they enter the food chain (Hassoun and Emir Çoban 2017). Therefore, research on oil–water separation technology has practical importance, and many methodologies like mechanical oil boom (Etkin and Nedwed 2021), in situ burning of oil (Faksness et al. 2022), oil spill remediation dispersants (John et al. 2016), biodegradation technology (Xue et al. 2015) and oil-absorbing materials (Zhang et al. 2019) have been extensively investigated for the removal of oil pollutants from water bodies. Among these methods, porous oil-absorbing materials are considered highly promising for oil–water separation applications due to their low-cost, short treatment period, absence of secondary contamination and the possibility of oil recycling (Hao et al. 2019; Deng et al. 2020; Liu et al. 2021). These commonly used porous materials for oil–water separation including activated carbon, resin sponges, cotton fabrics and aerogels (Wang et al. 2022; Sun et al. 2021; Rana et al. 2016). Herein, melamine formaldehyde resin sponge (MFRS) possesses numerous attractive advantages, such as chemical and mechanical durability, porous and lightweight, environmentally friendly features,

✉ Litao Ma
malitaowj@163.com

[1] CNOOC Experimental Center, CNOOC Ener Tech-Drilling & Production Co., Tianjin 300452, China

[2] Shaanxi Key Laboratory of Advanced Stimulation Technology for Oil and Gas Reservoirs, Xi'an Shiyou University, Xi'an 710065, China

etc. (Wang et al. 2023). However, these porous materials are mostly hydrophilic, hence demonstrating very low efficiency in oil–water separation.

Nanostructure modification and chemical modification of surfaces have been widely studied to develop porous materials with hydrophobic and lipophilic properties for efficient oil–water separation. Nanostructure modification is achieved by the construction of geometric folds on the surfaces of materials to hinder the infiltration of water droplets into the materials, thereby improving their hydrophobicity (Wu et al. 2019; Chu et al. 2023). Meanwhile, chemical modification of surfaces involves procedures that alter the surface chemistry of materials to introduce new functionalities, characteristics and performances to the materials (Wang et al. 2020; Pan et al. 2021; Jing et al. 2023). The principle for the chemical modification of surfaces to improve the hydrophobicity of materials is based on the introduction of compounds containing hydrophobic functional groups with low surface energy (Shi et al. 2022). Compounds that commonly contain hydrophobic functional groups include fluoropolymers, silane coupling agent, polydopamine and oil (Lv and Cheng 2021; Zhang et al. 2022). Oils containing hydrophobic functional groups, such as polydimethylsiloxane (PDMS), do not only exhibit hydrophobic properties, but also display lipophilicity. PDMS-modified porous materials have received extensive research interest in oil–water separation applications owing to their inexpensive nature, as well as their chemical and mechanical stability (Liu et al. 2019). Jin et al. (2015) prepared PDMS/cotton via a solution-immersion process and achieved a water contact angle greater than 157°. Wang and coworkers (Wang et al. 2019) fabricated PDMS@starch coatings for effective separation of oil–water mixture and emulsions, and investigations confirmed its strong hydrophobicity. Chen et al. (2016) modified sponges with PDMS via a solution-immersion process and attained efficient separations of hexane, toluene, octadecene, silicone oil and motor oil from an oil–water mixture. Chu et al. (2022) synthesized PDMS/cellulose nanofiber by an electroless deposition method, and the material exhibited an oil absorption capacity greater than 60% of its volume. However, the weak chemical bonds between the porous materials and PDMS resulted in reduced selectivity for oil–water separation in recycling experiments. This is a limitation for the practical application of this method.

To resolve this problem, porous materials modified with PDMS-based coatings were developed to improve the durability and recyclability of the modified material by introducing more functional blocks. Tong et al. (2022) synthesized a porous rGO/PEI/PDMS sponge in six steps and achieved excellent recyclability due to the enhancement of the interface interaction between the rGO and PDMS by PEI as the adhesive layer. Moreover, Wen et al. (2021) reported a progressive graft polymerization method for the sequential introduction of functional glycidyl methacrylate (GMA), diethylenetriamine (DETA) and PDMS block on the surface of cotton fabrics, and the resulting material displayed satisfactory recyclability and stability in oil–water separation. However, such a step-by-step grafting process is often tedious, signifying low operational feasibility and discouraging large-scale applications. This drawback became the major motivation for the current study. We therefore designed and synthesized a PDMS-based copolymer containing various functional parts, and the porous material (such as MFRS) was modified by copolymers via a one-step method. Interestingly, the constituent acrylate double bond and epoxy group in glycidyl methacrylate (GMA) played significant roles in the fabrication process. While the acrylate double bond was co-polymerized with PDMS, the epoxy group reacted with a variety of functional groups to form firm chemical bonds. Hence, the PDMS-PGMA copolymer exhibited promising potentials for practical applications.

Herein, we synthesized a PDMS-PGMA copolymer whose chemical structure was confirmed by ^{1}H NMR and FT-IR spectra. Then, we modified melamine formaldehyde resin sponges (MFRS) with PMMA, PDMS-PMMA or PDMS-PGMA via a simple solution-immersion. Furthermore, we compared the water contact angle (WCA) and oil–water separation efficiency of the modified MFRS. Moreover, the elastic property and geometry morphology of the PDMS-PGMA/MFRS were investigated. Benefiting from the introduction of functional blocks in the PDMS-PGMA copolymer, PDMS-PGMA/MFRS exhibited efficient capabilities for the separation of oil–water mixture. Finally, we provided explanations for the decrease in the separation efficiency of PDMS-PGMA/MFRS in recycling experiments. We believe that this work will inspire the fabrication of recyclable, durable, and efficient oil–water separation porous materials.

Experimental section

Materials

Melamine formaldehyde resin sponge (MFRS, Sichuan Super Poly New Material Co., Ltd.), *N*, *N*-dimethylformamide (DMF, Tianjin Fuyu Fine Chemical Co., Ltd., AR), plant oil (Yihai Kerry Arawana Holdings Co., Ltd.), polydimethylsiloxane (PDMS-OH, Laizhou Xintai Chemical Co., Ltd., CP), triethylamine (TEA, Tianjin Fuyu Fine Chemical Co., Ltd., AR), 4-dimethylaminopyridine (DMAP, Shanghai Fuzhe Chemical Co., Ltd., AR), 2-bromoisobutyryl bromide (BiBB, Shanghai Darui Fine Chemicals Co., Ltd., AR), dichloromethane (CH_2Cl_2, Tianjin Fuyu Fine Chemical Co., Ltd., AR), sodium bicarbonate ($NaHCO_3$, Shanghai Hongguang Chemical Factory, AR), cuprous chloride (CuCl,

Tianjin Dengfeng Chemical Reagent Factory, AR), magnesium sulfate anhydrous ($MgSO_4$, Shanghai Shanpu Chemical Co., Ltd., AR), *N*,*N*,*N*′,*N*′-tetramethylethylenediamine (TMEDA, Sinopharm Chemical Reagent Co., Ltd., AR), methanol (CH_3OH, Tianjin Damao Chemical Reagent Factory, AR) and glycidyl methacrylate (GMA, Aladdin, AR) were straightway used without purifications.

Tetrahydrofuran (THF, Tianjin Hedong District Hongyan Reagent Factory, AR) and cyclohexanone (CYC, Tianjin Chemical Reagent Sixth Factory, AR) were purified by adding calcium hydride to solutions under magnetic stirring for 24 h, respectively, followed by distilling of the reaction solution and collecting the distilled liquid.

Synthesis of copolymers

The copolymers of both PDMS-PGMA and PDMS-PMMA were synthesized by similar procedures, the synthesis steps of PDMS-PMMA are described in detail in previous work (Niu et al. 2014), and the PDMS-PGMA was synthesized in the following steps.

Firstly, we have prepared the PDMS-Br. A Schlenk flask was pumped out of the air and fed with N_2 in an ice-bath, and the THF solutions of PDMS-OH, TEA and DMAP were introduced under the protection of N_2. Followed by addition of a certain amount of BiBB solution, and then the reaction was carried out at room temperature under magnetic stirring for 24 h to obtain a white suspension. After that, the suspension was removes large particles by centrifugation and filtration, and the THF solution was removed by rotary evaporation to obtain the crude products. Next, the crude products were redissolved in CH_2Cl_2, washed with saturated $NaHCO_3$ solution and dried with anhydrous $MgSO_4$, before performing filtering operations. Lastly, the PDMS-Br was obtained after conducting rotary evaporation to remove CH_2Cl_2.

Subsequently, pre-determined amounts of CuCl were transferred to a Schlenk flask, the air in Schlenk flask was pumped out and replaced by N_2. The cyclohexanone solutions of PDMS-Br, TMEDA and GMA (quality of GMA/PDMS-Br = 10:1) then introduced to the above-mentioned Schlenk flask; it was reacted under magnetic stirring at 80 °C for 24 h. After natural cooling to 50 °C, the reaction mixture was conducted dilute by THF, filtering operations to remove Cu^{2+} and rotary evaporation to remove THF, followed by precipitation of solid products via addition of the aforementioned mixture into methanol. Finally, the PDMS-PGMA copolymer powder was obtained after drying the collected solid products.

Modification of MFRS

In this paper, a solution-immersion process (Camalan and İhsan Arol 2022) was used to functionalize MFRS; we used PMMA, PDMS-PMMA and PDMS-PGMA to modify MFRS, respectively. The procedure for sponge modification is basically similar, and the PDMS-PGMA-modified melamine formaldehyde resin sponge (PDMS-PGMA/MFRS) was fabricated as follows. Firstly, the homogeneous polymer solution was prepared by sufficient disperse 2.5 g PDMS-PGMA powder in 50 mL DMF. Then, the tailored MFRS (length × width × height = 6 cm × 2.5 cm × 2 cm) was completely immersed in the aforementioned polymer solution for 1 h. After that, the excess solution in MFRS is squeezed out and the sponge is placed in an oven to performing fully dry treatment.

Elasticity performance test of MFRS

Firstly, the initial height of the modified and unmodified sponge was measured by a ruler. Then, apply a ceramic sheet to compress the sponge to 1/4 of its original height, and 10 s later, the ceramic sheet was removed slowly. The height was recorded after the sponge was restored to its original shape in 5 min. To assess the elastic properties of sponge, the above operation is repeated for 10 times.

Oil/water separation experiment of MFRS

Oil/water mixture were prepared by introducing 15 mL plant oil to 85 mL DI water and processing 30-min ultrasonic treatment. Then, the modified or unmodified sponges were transferred to a conical flask containing 100 mL oil/water mixture. After that, the conical flask was placed in a running thermostatic shaker for 10 min oil/water separation. Following by remove the sponge and calculate oil/water separation efficiency by measure the volume of water and oil in separated solution. η_{Water} is the calculated ratio of the volume of water after separation to the initial volume of water, and η_{Oil} is the calculated ratio of the volume of oil that absorbed by sponge to the initial volume of oil; the formula is as follows.

$$\eta_{Water} = V_1/V_2 \times 100\%$$
$$\eta_{Oil} = \left(V_4 - V_3\right)/V_4 \times 100\%$$

where V_1 and V_3 represent the volume of water and oil in the separated solution, while V_2 and V_4 refer to the volume of water (85 mL) and oil (15 mL) in the initial oil–water mixture.

Meanwhile, to evaluate the influence of pH on the oil–water separation efficiency of PDMS-PGMA/MFRS, the PDMS-PGMA/MFRS was immersed in alcohol solutions of pH = 1, 4, 10, 13 for 24 h, respectively, before conducting oil–water separation experiments.

Furthermore, to assess the recyclability of PDMS-PGMA/MFRS, the modified sponges squeezed out the adsorbed oil

and washed for five times with alcohol after each use. Then, the used PDMS-PGMA/MFRS is dried for reuse.

Characterization

An OCA20 contact angle goniometer (Data Physics, Germany) was used to measure water contact angle (WCA) of accurate 300 µL DI water droplets on modified MFRS exposed to air. The chemical structures of unmodified and modified MFRS were obtained using a Tensor 27 of Bruker Optics in a FT-IR spectrometer for spectral range 400–4000 cm^{-1}. A JEOL 7800F Field Emission Scanning Electron Microscope was used to obtain SEM images of MFRS before modified and modified by PDMS-PGMA. A Bruker AV-500 spectrometer using (Methyl sulfoxide)-d6 or $CDCl_3$ as solvent was used to collect proton nuclear magnetic resonance (^{1}H NMR) data for obtained PDMS-PGMA copolymer. The electronic universal mechanical testing (CITEMA, Shanghai) was used to test the stress–strain curves of unmodified and PDMS-PGMA-modified MFRS as 0.01 mm s^{-1} squeezing speed.

Results and discussion

The chemical structure of the PDMS-PGMA copolymer was deduced by ^{1}H NMR spectrum, as shown in Fig. 1a. The chemical shift recorded at 0.1 ppm (a) and 1.8 ppm (b) was attributed to the Si–(C$\underline{H}_3$) and –C$\underline{H}_2$– of the PDMS block (Liang et al. 2011). Similarly, the peaks observed at 3.2 (d), 2.7 and 2.8 (f), 3.8 and 4.3 (e) ppm indicate the presence of epoxy group, and 0.9 ppm (c) belonging to –C$\underline{H}_3$ from GMA block, further confirming the existence of GMA repeat units in the copolymer (Hameed et al. 2010). Therefore, the ^{1}H NMR spectrum provided evidence for the successful synthesis of the PDMS-PGMA copolymer. Meanwhile, the ^{1}H NMR spectra of PDMS and PDMS-PMMA were investigated (Fig. S1). Compared to the chemical shift at 3.65 ppm (OH–C$\underline{H}_2$–CH_2–), 0.07 ppm (–Si(C$\underline{H}_3$)$_2$–O–) and 0.81 ppm (α-C$\underline{H}_2$ to the Si atom) from PDMS (Fig. S1a) (Subramanyam and Kenedy 2009; Li et al. 2013), some new peaks at 1.74, 1.85 and 3.55 ppm belonging to the protons of methyl, methylene and methoxy in PMMA chain (Li et al. 2013) can be clearly observed (Fig. S1b), which provided direct evidence of successful synthesis of PDMS-PMMA copolymer.

Moreover, Fourier transform infrared spectrometer (FT-IR) spectra were used to study functional groups of MFRS, PDMS-PGMA and PDMS-PGMA/MFRS (Fig. 1b). The signals of melamine formaldehyde resin sponge (MFRS) observed at 3424 cm^{-1} (N–H and O–H), 2959 cm^{-1} (C–H), 1688 cm^{-1} (C=N), 809 cm^{-1} (triazine ring) and 999 cm^{-1} (–CH_2OH) confirmed that MFRS is condensed from hydroxymethyl melamine (Xiong et al. 2020). Similarly, in PDMS-PGMA copolymer, the absorption bands recorded at 800 cm^{-1} (C–Si–C) and 1091 cm^{-1} (Si–O–Si) verified the existence of PDMS (Hameed et al. 2010), while the signals at 1727 cm^{-1} (C=O) and 906 cm^{-1} (epoxy group) validated the introduction of GMA block in the copolymer (Zhou et al. 2019). Besides, the absorption bands of PDMS-PGMA/MFRS were similar to those of PDMS-PGMA, which was ascribed to the sufficient coating of PDMS-PGMA on MFRS.

Furthermore, the chemical structure of PDMS-PMMA/MFRS was further investigated by FT-IR spectrum in Fig.

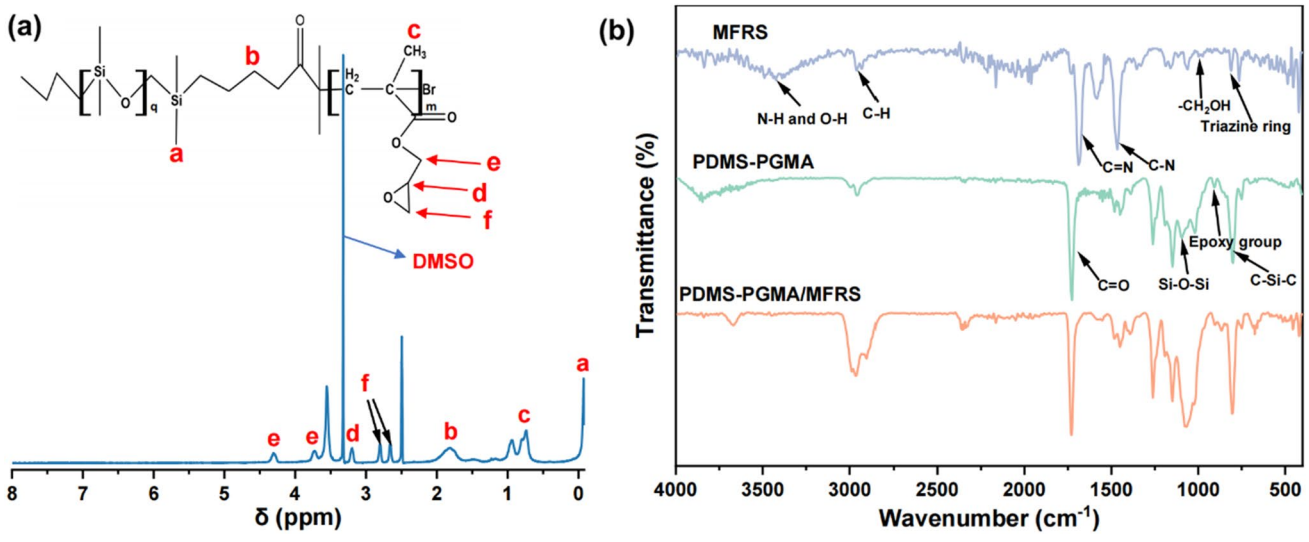

Fig. 1 **a** ^{1}H NMR spectrum of PDMS-PGMA copolymer (Inset—the chemical structure of PDMS-PGMA). **b** FT-IR spectra of MFRS, PDMS-PGMA copolymer and PDMS-PGMA/MFRS

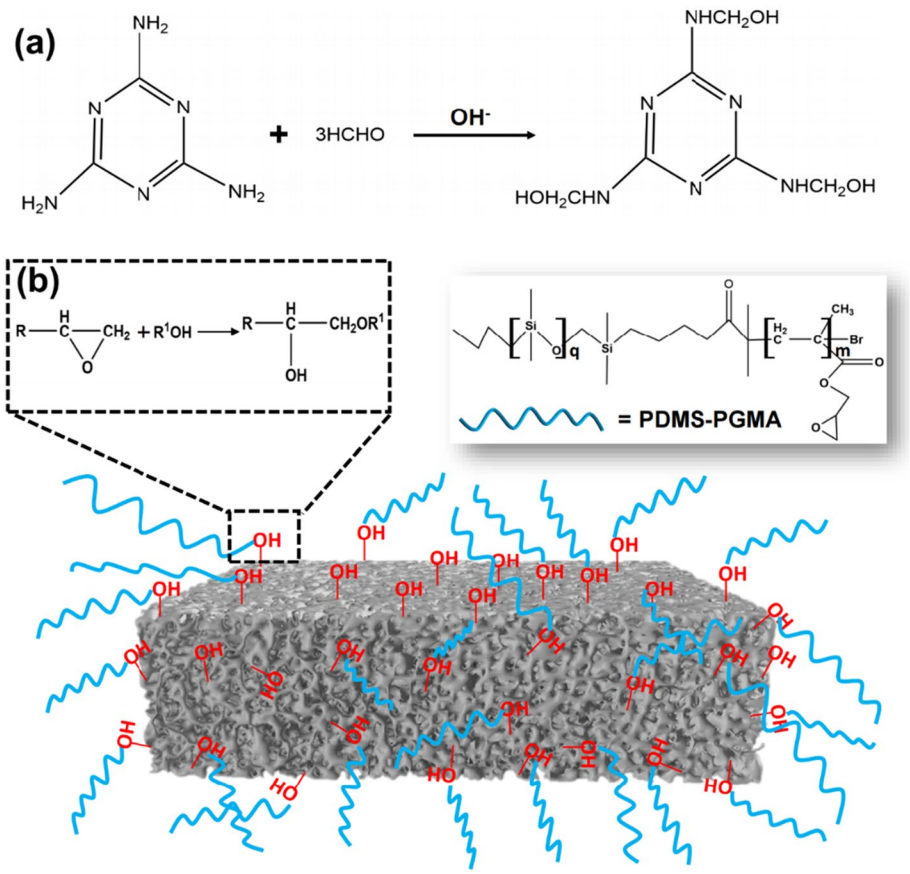

Scheme 1 **a** Scheme diagram of additive reaction in synthesis melamine formaldehyde resin. **b** Schematic diagram of modification of MFRS by PDMS-PGMA copolymer

S2. Apart from the absorption bands at 3429 cm^{-1} (N–H and O–H), 2964 cm^{-1} (C–H), 1454 cm^{-1} (C–N) and 815 cm^{-1} (triazine ring) from MFRS (Chen et al. 2008), the signals observed at 1737 cm^{-1} (C=O) and 1016/1099 cm^{-1} (Si–O–CH_3) were derived to the PMMA and PDMS block of PDMS-PMMA, respectively, further confirming the chemical structure of PDMS-PMMA/MFRS.

The major composition of the sponge is melamine formaldehyde resin, which was synthesized by an additive reaction between formaldehyde and melamine, followed by a condensation reaction. Hydroxymethyl melamine was obtained in the additive reaction (Scheme 1a), and the subsequent condensation reaction partially removed water, while adequate amounts of hydroxyl groups were still retained [as confirmed by FT-IR spectra: 3424 cm^{-1} (O–H), 999 cm^{-1} (–CH_2OH)]. These hydroxyl groups were available for reaction with the epoxy groups, thereby leading to the grafting of the PDMS-PGMA copolymer on MFRS (Scheme 1b), which was further confirmed by the FT-IR spectra of MFRS and PDMS-PGMA/MFRS (Fig. 1). Interestingly, the PGMA block of PDMS-PGMA bonded with MFRS to form a stable coating, and the PDMS block afforded superhydrophobic properties on MFRS.

In order to investigate the elastic properties of the sponges modified by the polymers, we compared the elastic property data of the unmodified MFRS with those of the modified MFRS (PDMS-PGMA/MFRS), as shown in Fig. 2. The original heights of both the MFRS and PDMS-PGMA/MFRS were 2.00 cm (Fig. 2a, b), and the sponges were squeezed to 1/4 of their original heights (Fig. 2a1 and b1). PDMS-PGMA/MFRS was restored to 97.5% of its original height after fivefold squeezing and 96.5% after tenfold squeezing (Fig. 2c). Meanwhile, stress–strain curves were performed to investigate the elastic property of MFRS and PDMS-PGMA/MFRS (Fig. S3). Compared with MFRS, PDMS-PGMA-modified MFRS demonstrated easier deformation under pressure (less than 50% of strain), suggesting a slightly reduced mechanical property after coating. However, the final stress–strain result of PDMS-PGMA/MFRS displayed same stress with pure MFRS, possible due to the unchanged structure of sponge, which was consistent with the conclusions from elasticity performance test. Therefore, we believed that PDMS-PGMA/MFRS did not suffer a significant decrease in elastic performance in comparison with the pure MFRS, indicating that the modified sponge exhibited an excellent elastic property, hence demonstrating its reusability potential.

Scanning electron microscope (SEM) was used to investigate the geometry morphology of MFRS and PDMS-PGMA/MFRS, and the micrographs are displayed in Fig. 3.

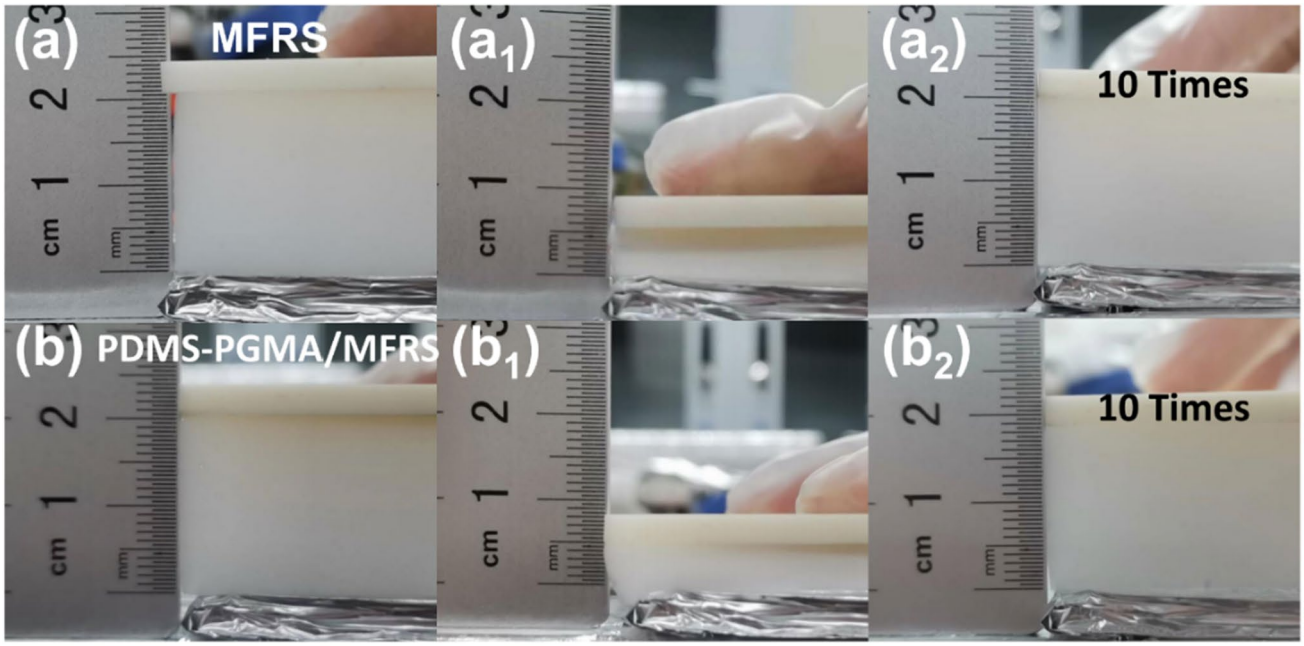

(c)

Compressions number		0	1	2	3	4	5	6	7	8	9	10
Sponge height (cm)	MFRS	2.00	1.97	1.97	1.96	1.96	1.95	1.95	1.95	1.95	1.95	1.95
	PDMS-PGMA/MFRS	2.00	1.97	1.95	1.95	1.95	1.95	1.94	1.94	1.94	1.93	1.93

Fig. 2 Images of **a** unmodified (MFRS) and **b** PDMS-PGMA-modified MFRS in elastic properties testing procedure. $\mathbf{a_1}$ and $\mathbf{b_1}$ Sponge compression process, $\mathbf{a_2}$ and $\mathbf{b_2}$ images of unmodified (MFRS) and PDMS-PGMA-modified MFRS after 10 times of elastic properties testing. **c** Elastic properties of unmodified and PDMS-PGMA-modified MFRS

Both the surface and internal section of MFRS presented a porous structure, with an average pore size of nearly 100 µm (Fig. 3a, b), and the appearance presented a smooth and regular feature (Fig. 3a2, b2). Furthermore, the three-dimensional structure of PDMS-PGMA/MFRS is similar to that of MFRS (Fig. 3c, d), suggesting that the polymer modification did not change the porous structure of MFRS. However, the appearance of the PDMS-PGMA-modified MFRS was rough and wrinkled (Fig. 3c2, d2), which is attributed to the polymer coating on MFRS. Wrinkles were observed on both the surface and internal section of PDMS-PGMA/MFRS, indicating the successful modification of MFRS by PDMS-PGMA. Therefore, the geometric wrinkles on the PDMS-PGMA/MFRS surface and the introduced functional groups may have enhanced the hydrophobic properties of MFRS (Zou et al. 2017; Kieu et al. 2019).

We evaluated the corresponding hydrophobicity and water contact angle (WCA) images to compare the hydrophobic properties of the different modified MFRS (Fig. 4). The water droplets were rapidly absorbed on MFRS (Fig. 4e, e1), indicating that MFRS had a strong hydrophilicity, which was probably related to the presence of the hydroxyl groups on the surface of MFRS. Meanwhile, PMMA-modified MFRS exhibited non-uniform hydrophobic properties (Fig. 4e, e2), implying that while hydrophobicity dominated some areas, hydrophilicity characterized the other areas. The WCA values were 126° on the surface of PMMA/MFRS and 61° in the internal section (Fig. 4a) due to the poor adhesion and uneven dispersion of the PMMA coating. However, PDMS-PMMA-modified MFRS exhibited improved WCA with 139° for the surface and 134° for the internal section (Fig. 4b). The enhanced hydrophobic performance may have been influenced by the introduction of the PDMS block (Moquin et al. 2018). Besides, the PDMS-PGMA-modified MFRS demonstrated superhydrophobic properties with WCA of 155° on the surface (Fig. 4c). Such a result was probably influenced by the presence of the hydrophobic groups of PDMS together with the geometric folds formed by the copolymer on MFRS.

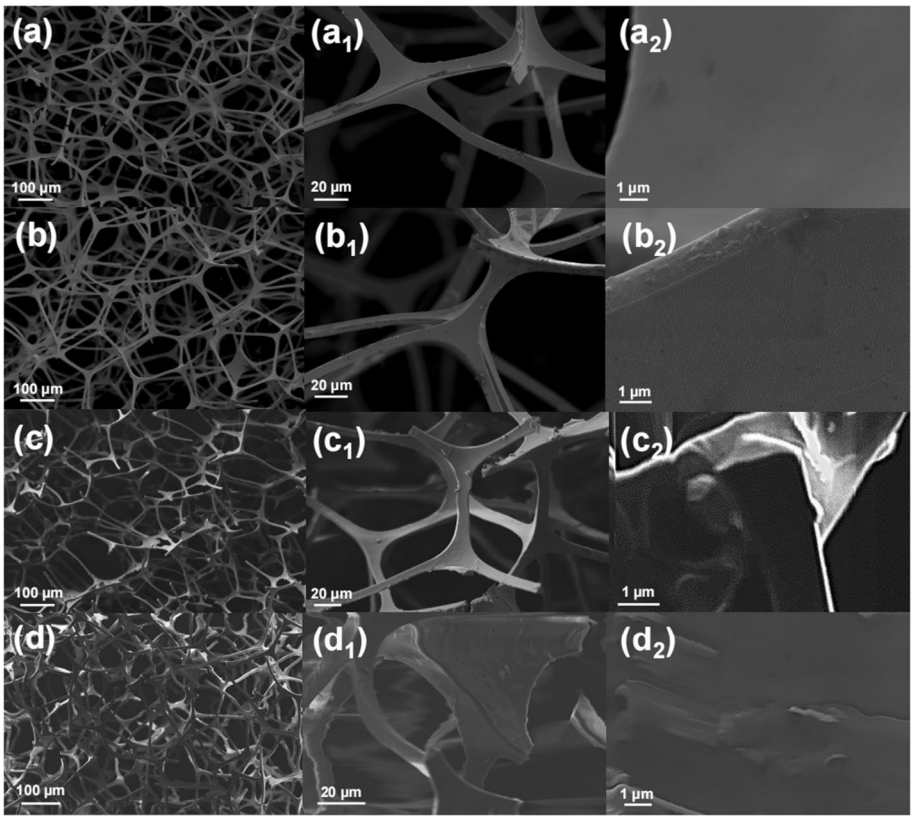

Fig. 3 Different resolution SEM images of MFRS: **a**–**a**$_2$ surface and **b**–**b**$_2$ internal section. Different resolution SEM images of PDMS-PGMA/MFRS: **c**–**c**$_2$ surface and **d**–**d**$_2$ internal section

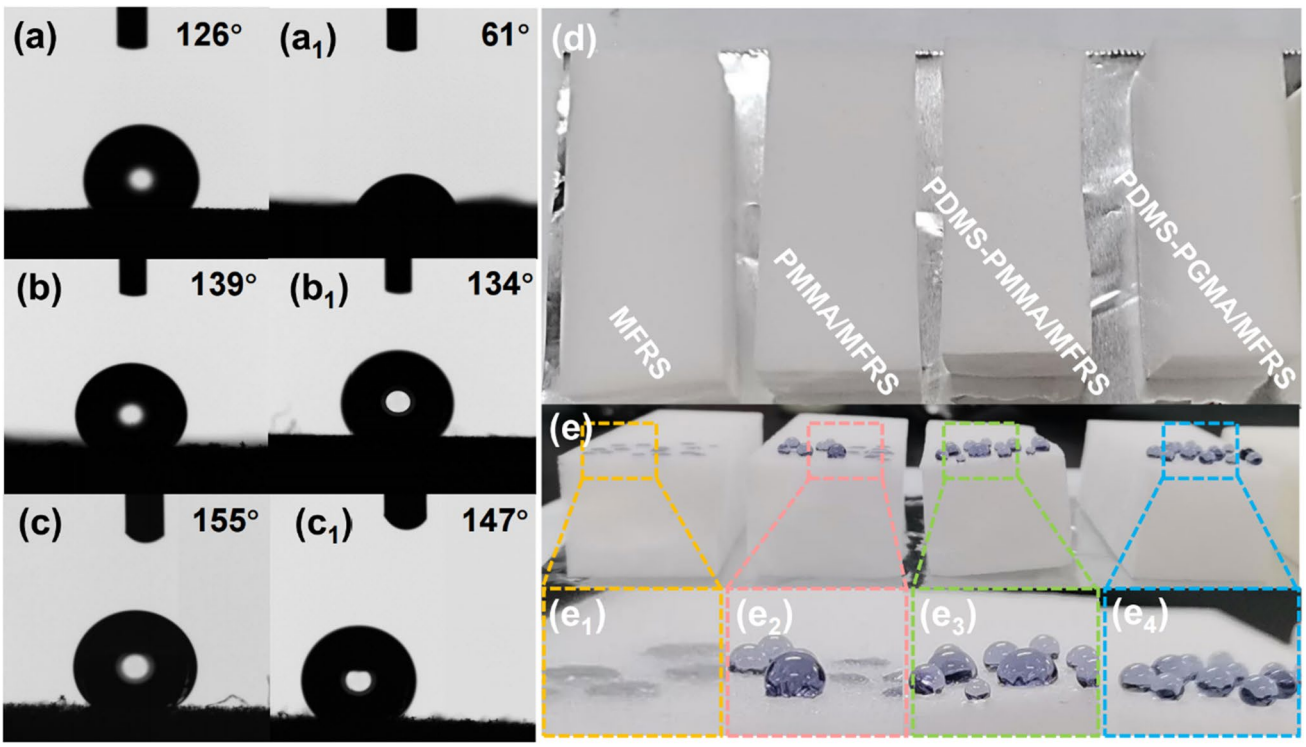

Fig. 4 Water contact angle (WCA) images of PMMA/MFRS (**a**–**a**$_1$ surface and internal section), PDMS-PMMA/MFRS (**b**–**b**$_1$ surface and internal section) and PDMS-PGMA/MFRS **c**–**c**$_1$ surface and internal section). **d** and **e** Hydrophobic images of MFRS modified by different polymers, and high-resolution hydrophobic images of **e**$_1$ MFRS, **e**$_2$ PMMA/MFRS, **e**$_3$ PDMS-PMMA/MFRS, and **e**$_4$ PDMS-PGMA/MFRS

To assess the oil–water separation efficiency of the different polymer-modified MFRS, uniform-sized blocks (length × width × height = 6 cm × 2.5 cm × 2 cm) were loaded in a conical flask with oil–water mixture (Fig. 5a, b). The pure MFRS sank to the bottom of the conical flask upon transfer to the mixture, suggesting excellent hydrophilicity. This was followed by the transfer of the aforementioned conical flask to a water bath shaker which was operated for 10 min. After the shaking process, MFRS, PMMA/MFRS and PDMS-PMMA/MFRS sank to the bottom of the conical bottle, and the oil–water mixture presented a cloudy appearance (Fig. 5c, d). However, the MFRS modified by PDMS-PGMA floated on the liquid surface, indicating that its excellent hydrophobic property was maintained, and the separated oil–water mixture was clear in appearance (Fig. 5d). This may be ascribed to the preoccupation of the pores of the modified MFRS with oil due to the interaction of the capillary and Van Der Waals forces, while water was repelled (Li et al. 2018).

The separation efficiency of the MFRS modified with different polymers was denoted by η_{Oil} and η_{Water}, where the level of η_{Oil} and η_{Water} reflect the lipophilicity and hydrophobicity of MFRS, respectively. The separation efficiency represented by η_{Water} (70.6%) and η_{Oil} (40.0%) exhibited a significant gap for pure MFRS (Fig. 6a), which is attributed to its non-selective absorption of oil–water mixtures. In contrast, the values of η_{Water} and η_{Oil} were quite similar for PMMA/MFRS, PDMS-PMMA/MFRS and PDMS-PGMA/MFRS, indicating that the lipophilicity and hydrophobicity of the materials are related (Liao et al. 2021). Compared to PMMA/MFRS, PDMS-PMMA/MFRS demonstrated a higher oil–water separation efficiency, which is ascribed to the enhanced hydrophobic performance by the introduction of PDMS block. Moreover, PDMS-PGMA-modified MFRS demonstrated desirable oil–water separation efficiency, with η_{Water} of 98.8% and η_{Oil} of 99.3%. These reflect favorable hydrophobic properties, which may have been influenced by both the introduction of hydrophobic PDMS block and the tight bonding of PGMA block with MFRS.

Reusability is an important parameter for the performance evaluation of oil–water separation. The separation efficiency (η_{Water}) of PDMS-PGMA/MFRS after 4 runs was 96.5%, and 91.5% after 8 runs (Fig. 6b). The volume of PDMS-PGMA/MFRS was significantly reduced after 8 runs (Fig. 6c), whereas its hydrophobicity was still retained (Fig. 6d3). Furthermore, acid and alkali resistance are an important factor in evaluating hydrophobic materials. The PDMS-PGMA/MFRS material was immersed for 24 h in alcohol solutions with different pH, followed by drying prior to oil–water separation experiments. The oil–water separation efficiency (η_{Water}) displayed a decreasing trend with increasing or decreasing pH (Fig. 6e). The PDMS-PGMA/MFRS exhibited an oil–water separation efficiency of 98.7% after immersion in an unadjusted alcohol solution, and the value was 94.7% for the solution at pH = 1. PDMS-PGMA/MFRS was more unstable in strong bases compared with strong

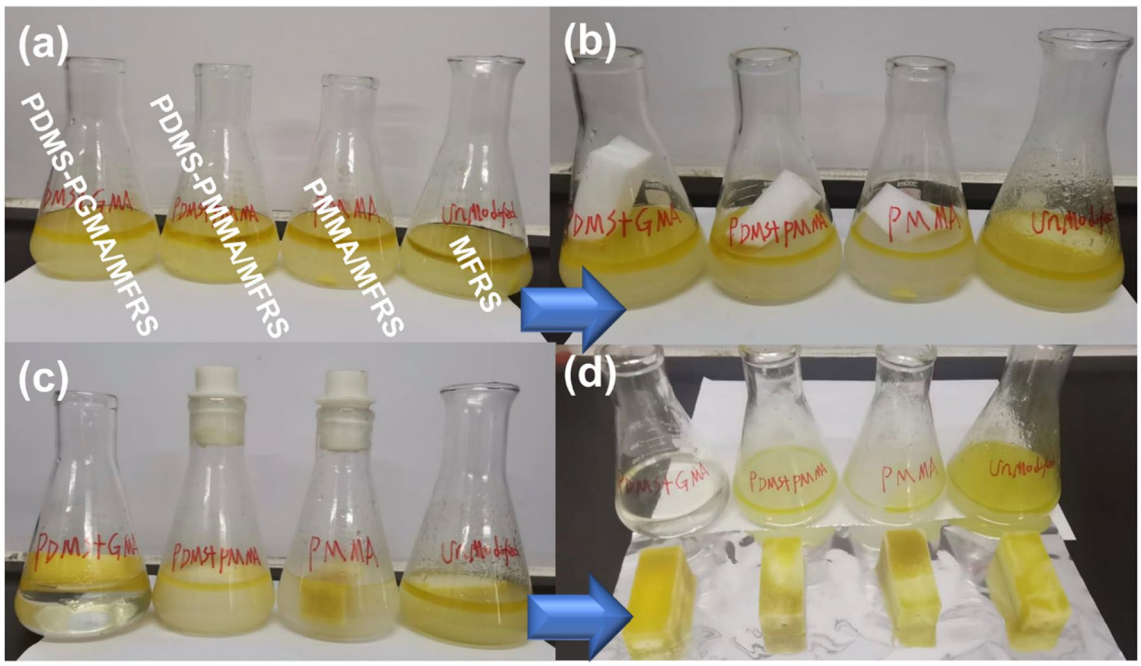

Fig. 5 **a** Images of oil–water mixture before separation and **b** the loading of different polymer-modified MFRS into oil–water mixtures. **c** Images of different polymer-modified MFRS in oil–water mixture after separation. **d** Images of oil–water mixture and sponges after separation

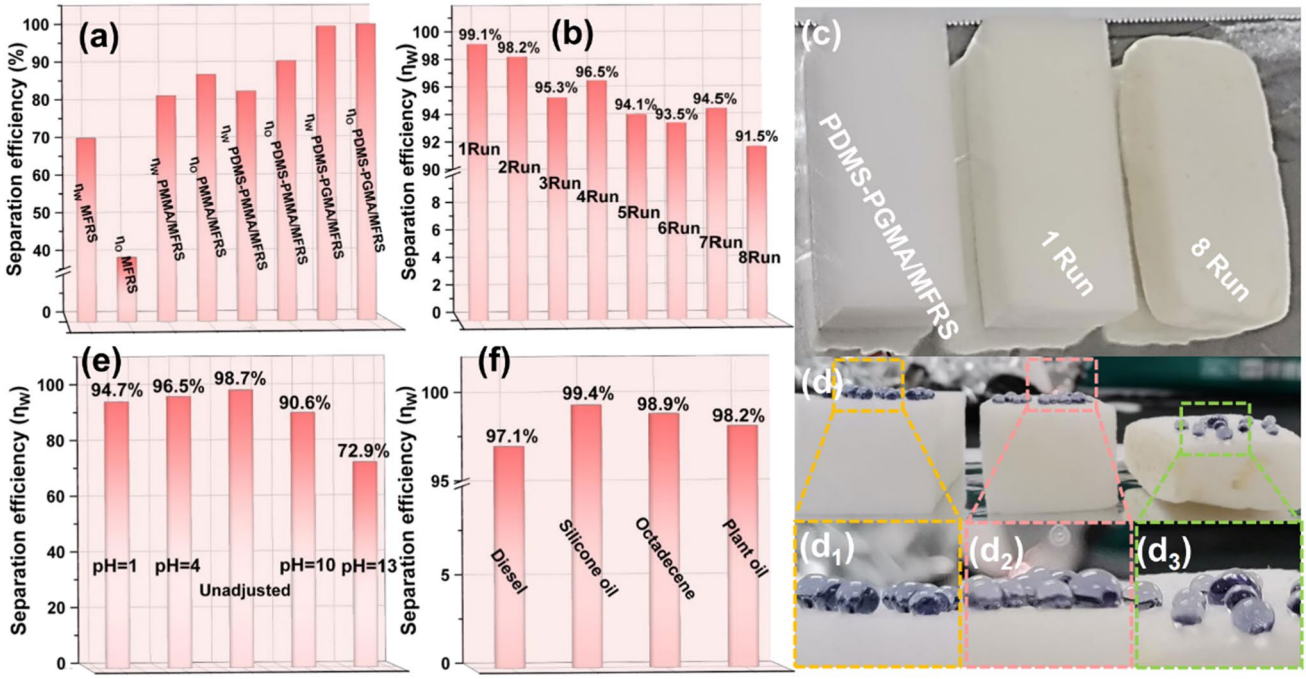

Fig. 6 **a** Oil–water mixture separation efficiency of MFRS modified with different polymers. **b** Recyclability of PDMS-PGMA/MFRS. **c** Actual and **d** hydrophobic images of PDMS-PGMA/MFRS $\mathbf{d_1}$ before use, $\mathbf{d_2}$ after 1 run and $\mathbf{d_3}$ 8 runs. **e** Acid/alkaline resistance capability of PDMS-PGMA/MFRS. **f** Separation efficiency of PDMS-PGMA/MFRS for different oil–water mixtures

acids, which is reflected by the 72.9% separation efficiency after immersion in an alcohol solution of pH = 13. Therefore, PDMS-PGMA/MFRS exhibited strong acid resistance and weak alkali resistance, which is attributed to the destruction of the hydrophobic functional groups and chemical bonds between the copolymers and MFRS by strong base solutions (Cui and Liu 2021). Besides, PDMS-PGMA/MFRS achieved efficient separation of different types of oil–water mixtures. The separation efficiencies (η_{Water}) were 97.1%, 99.4%, 98.9% and 98.2% for diesel-water, silicone oil–water, octadecene–water and plant oil–water mixture, respectively (Fig. 6f). Therefore, based on the above-mentioned discussion, the recyclability, acid resistance and effective separation for different oil–water mixtures of PDMS-PGMA/MFRS demonstrate the potential of the material for practical applications.

FT-IR was used to investigate the functional group variations of PDMS-PGMA/MFRS before and after oil–water separation (Fig. 7a). Peak signal enhancement occurred around 2800–3000 cm^{-1} (C–H) after oil–water separation measurements. Also, a new peak appeared at 720 cm^{-1} ($-(CH_2)_n-$, $n > 4$) after 1 run and 8 runs (Guo and Bustin 1998; Huang and Wang 2009). The enhanced signal and new peak appearance are confirmations of the adsorption of long-chain alkanes on the surface of PDMS-PGMA/MFRS. Moreover, we observed that some absorption bands of PDMS-PGMA/MFRS disappeared or were diminished after 1 run and 8 runs of separation, such as 1260 cm^{-1} (C–O), 1080 cm^{-1} (Si–O–Si) and 802 cm^{-1} (C–Si–C) all belonging to the signals of the PDMS block (Zhou et al. 2019). These disappeared or diminished signals should have been masked by the adsorbed alkanes, further suggesting that the PDMS block plays hydrophobic and lipophilic functions in oil–water separation. The WCA of PDMS-PGMA/MFRS slightly decreased on both the surface (151°) and internal section (136°) after 1 run of oil–water separation (Fig. 7b, b1). Similarly, the WCA values were recorded as 135° on the surface and 130° on the internal section after 8 runs of separation (Fig. 7c, c1). Meanwhile, the SEM images of PDMS-PGMA/MFRS after 8 runs of separation exhibited some breakages in sponge connectivity (Fig. 7d, d1), possibly due to the physical overuse and damage after squeezing during oil absorption and discharge processes, which may be the direct reason for the decrease in sponge volume. However, traces of the copolymer were still clearly observed on the surface of MFRS (Fig. 7d2) and are the main contributor to the hydrophobicity of MFRS. Therefore, the decreased oil–water separation efficiency in the recycling experiment should attributed to the combined effect of the declined volume of MFRS and the diminished hydrophobicity of the modified copolymer.

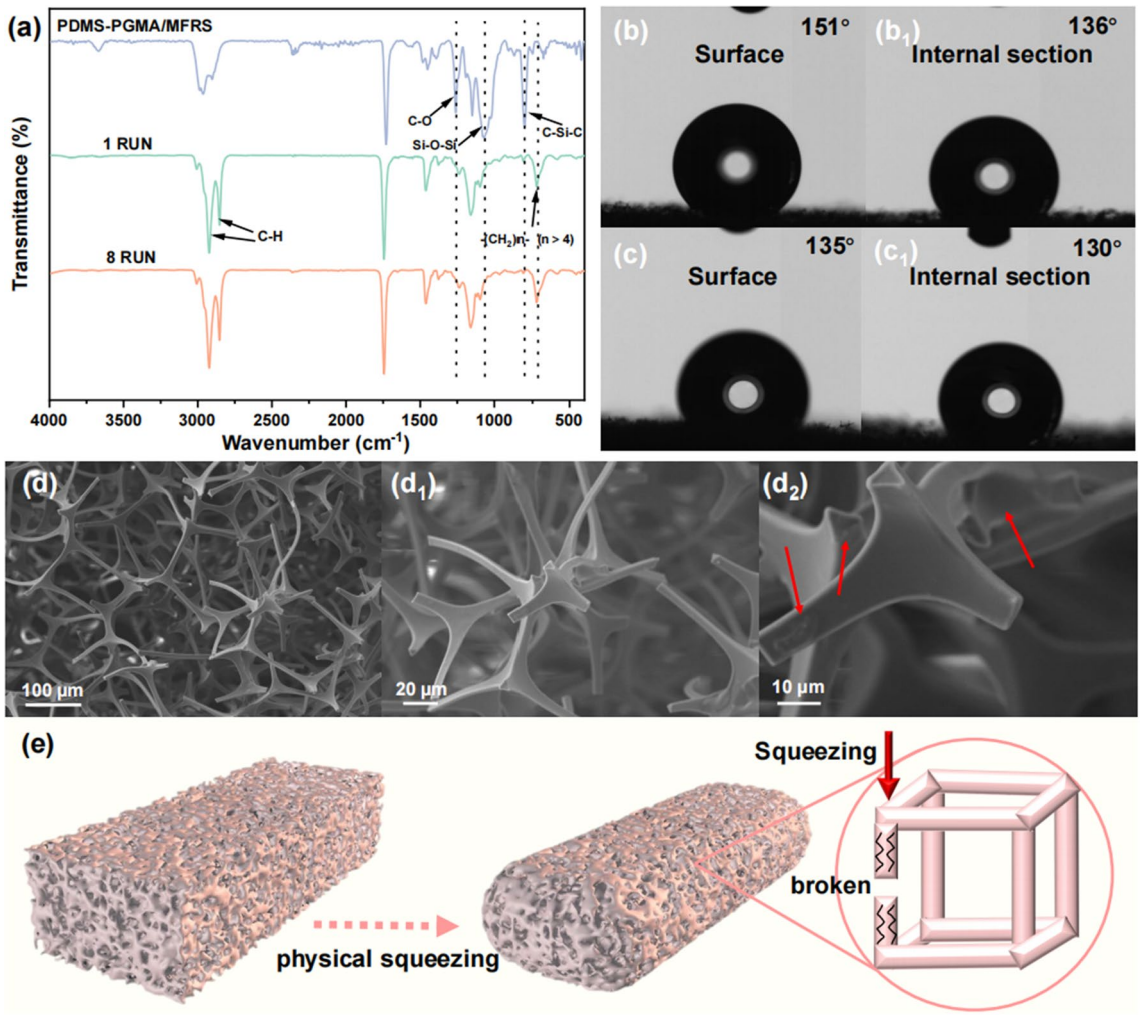

Fig. 7 **a** FT-IR spectra of PDMS-PGMA/MFRS sample before and after oil–water separation. WCA images of PDMS-PGMA/MFRS after **b** 1 run and **c** 8 runs of oil–water separation. **d** SEM images of PDMS-PGMA/MFRS after 8 runs of oil–water separation. **e** Schematic diagram for reduced sponge volume in recycling experiments

Conclusion

In summary, we report the synthesis of PDMS-PGMA copolymer, followed by the fabrication of PMMA, PDMS-PMMA and PDMS-PGMA-modified MFRS via a facile solution-immersion process. PDMS-PGMA/MFRS demonstrated superhydrophobicity with WCA values of 155° and 147° on its surface and internal section, respectively. The superhydrophobic property of PDMS-PGMA/MFRS was attributed to both the introduction of hydrophobic PDMS fragments and the geometric fold structures induced by the copolymer coating. Benefiting from the hydrophobicity, PDMS-PGMA/MFRS exhibited efficient oil-absorbing ability in oil–water mixture, which was reflected by the η_{Oil} value of 99.3%. Moreover, PDMS-PGMA-modified MFRS demonstrated favorable recyclability, with a separation efficiency of 91.5% after 8 runs, and this is attributed to the strong chemical bonds between MFRS and the epoxy group of GMA in the copolymer. Besides, PDMS-PGMA/MFRS displayed good acid resistance and was efficient in the separation of various oil–water mixtures. Thus, these promising results reflect the highly efficient, recyclable, acid-resistant and widely adaptable features of the fabricated PDMS-PGMA/MFRS, which shows possibilities for large-scale oil spill removal.

Supplementary Information The online version contains supplementary material available at https://doi.org/10.1007/s11696-023-03191-7.

Acknowledgements This work was primarily supported by the Project from China National Offshore Oil Corporation (CNOOC-KJ PT GCJS 2021-01) and the National Natural Science Foundation of China (NSFC Grants 51934005 and 52074226).

Declarations

Conflict of interest The authors declare no competing financial interest.

References

Amina H, Unnikrishnan G (2023) Bio-lubricants from vegetable oils: Characterization, modifications, applications and challenges—review. Renew Sustain Energ Rev 182:113413

Camalan M, İhsan Arol A (2022) Preliminary assessment of spray coating, solution-immersion and dip coating to render minerals superhydrophobic. Miner Eng 176:107357

Chen H, Deng X, Hou X, Luo R, Liu B (2008) Preparation and characterization of PDMS-PMMA interpenetrating polymer networks with indistinct phase separation. J Macromol Sci A 46:83–89

Chen X, Weibel J, Garimella S (2016) Continuous oil–water separation using polydimethylsiloxane-functionalized melamine sponge. Ind Eng Chem Res 55:3596–3602

Chu Z, Li Y, Zhou A, Zhang L, Zhang X, Yang Y, Yang Z (2022) Polydimethylsiloxane-decorated magnetic cellulose nanofiber composite for highly efficient oil–water separation. Carbohydr Polym 277:118787

Chu X, Zhang P, Shi S, Liu Y, Feng W, Zhou N, Li J, Shen J (2023) Hydrophobic self-cleaning micro–nano composite polyethylene-based agricultural plastic film with light conversion and abrasion resistance. Colloids Surf A Physicochem Eng Asp 658:130621

Cui C, Liu W (2021) Recent advances in wet adhesives: adhesion mechanism, design principle and applications. Prog Polym Sci 116:101388

Deng Y, Peng C, Dai M, Lin D, Ali I, Alhewairini S, Zheng X, Chen G, Li J, Naz I (2020) Recent development of super-wettable materials and their applications in oil–water separation. J Clean Prod 266:121624

Etkin DS, Nedwed TJ (2021) Effectiveness of mechanical recovery for large offshore oil spills. Mar Pollut Bull 163:111848

Faksness LG, Leirviket F, Taban I, Engen F, Jensen H, Holbu J, Dolva H, Bratveit M (2022) Offshore field experiments with in-situ burning of oil: emissions and burn efficiency. Environ Res 205:112419

Gryznova E, Davydov V, Grebenikova N, Puz'ko D, Karakotov S, Nadykta V, Ivanov D, Bykov V (2019) The study of the environmental efficiency of energy production from various sources of raw materials. IOP Conf Ser Earth Environ Sci 390:012044

Guo Y, Bustin R (1998) Micro-FTIR spectroscopy of liptinite macerals in coal. Int J Coal Geol 36:259–275

Hameed N, Guo Q, Xu Z, Hanley T, Mai Y (2010) Reactive block copolymer modified thermosets: highly ordered nanostructures and improved properties. Soft Matter 6:6119–6129

Hao W, Xu J, Li R, Zhao X, Qiu L, Yang W (2019) Developing superhydrophobic rock wool for high-viscosity oil/water separation. Chem Eng J 368:837–846

Hassoun A, Emir Çoban Ö (2017) Essential oils for antimicrobial and antioxidant applications in fish and other seafood products. Trends Food Sci Technol 68:26–36

Huang N, Wang J (2009) A TGA-FTIR study on the effect of $CaCO_3$ on the thermal degradation of EBA copolymer. J Anal Appl Pyrolysis 84:124–130

Jin Y, Jiang P, Ke Q, Cheng F, Zhu Y, Zhang Y (2015) Superhydrophobic and superoleophilic polydimethylsiloxane-coated cotton for oil–water separation process: an evidence of the relationship between its loading capacity and oil absorption ability. J Hazard Mater 300:175–181

Jing L, Yang P, Lu X, Tian H, Mao J, Li J, Ma F, Zhang Z (2023) Photochemical-initiated hydrophobic surface modification by benzophenone derivatives and its application on oil-water separation. Appl Surf Sci 608:155125

John V, Arnosti C, Field J, Kujawinski E, McCormick A (2016) The role of dispersants in oil spill remediation fundamental concepts, rationale for use, fate, and transport issues. Oceanography 29:108–117

Kieu H, Zhou K, Law A (2019) Surface morphology effect on the evaporation of water on graphene oxide: a molecular dynamics study. Appl Surf Sci 488:335–342

Li H, Liu S, Zhao J, Li D, Yuan Y (2013) Thermal degradation behaviors of polydimethylsiloxane-*graft*-poly(methyl methacrylate). Thermochim Acta 573:32–38

Li Q, Deng W, Li C, Sun Q, Huang F, Zhao Y, Li S (2018) High-flux oil/water separation with interfacial capillary effect in switchable superwetting $Cu(OH)_2$@ZIF-8 nanowire membranes. ACS Appl Mater Interfaces 10:40265–40273

Liang J, He L, Zhao X, Dong X, Luo H, Li W (2011) Novel linear fluoro-silicon-containing pentablock copolymers: synthesis and their properties as coating materials. J Mater Chem 21:6934–6943

Liao X, Sun D, Cao S, Zhang N, Huang T, Lei Y, Wang Y (2021) Freely switchable super-hydrophobicity and super-hydrophilicity of sponge-like poly(vinylidene fluoride) porous fibers for highly efficient oil/water separation. J Hazard Mater 416:125926

Liu J, Ye L, Wooh S, Kappl M, Steffen W, Butt H (2019) Optimizing hydrophobicity and photocatalytic activity of PDMS-coated titanium dioxide. ACS Appl Mater Interfaces 11:27422–27425

Liu S, Wang S, Wang H, Lv C, Miao Y, Chen L, Yang S (2021) Gold nanoparticles modified graphene foam with superhydrophobicity and superoleophilicity for oil–water separation. Sci Total Environ 758:143660

Lv J, Cheng Y (2021) Fluoropolymers in biomedical applications: state-of-the-art and future perspectives. Chem Soc Rev 50:5435–5467

Moquin A, Ji J, Neibert K, Winnik F, Maysinger D (2018) Encapsulation and delivery of neutrophic proteins and hydrophobic agents using PMOXA–PDMS–PMOXA triblock polymersomes. ACS Omega 3:13882–13893

Niu M, He L, Liang J, Pan A, Zhao X (2014) Effect of side chains and solvents on the film surface of linear fluorosilicone pentablock copolymers. Prog Org Coat 77:1603–1612

Pan A, Shi C, Jia M, He L (2021) Novel fluoroalkyl polyhedral oligomeric silsesquioxane (FPOSS) macromers for fabricating diblock copolymer as self-cleaning coatings. Prog Org Coat 151:106097

Rana M, Chen J, Yang S, Ma P (2016) Biomimetic superoleophobicity of cotton fabrics for efficient oil–water separation. Adv Mater Interfaces 3:1600128

Shi C, Zhang Y, Lu X, He Z, Pan A, Chang G, He L (2022) Highly-durable hydrophobic and adhesive coatings fabricated from graphene-grafted methacrylate copolymers. J Appl Polym Sci 139:e52917

Subramanyam U, Kenedy J (2009) PVA networks grafted with PDMS branches. J Polym Sci A Polym Chem 47:5272–5277

Sun R, Yu N, Zhao J, Mo J, Pan Y, Luo D (2021) Chemically stable superhydrophobic polyurethane sponge coated with ZnO/epoxy resin coating for effective oil/water separation. Colloids Surf A Physicochem Eng Asp 611:125850

Tong H, Chen H, Zhao Y, Liu M, Cheng Y, Lu J, Tao Y, Du J, Wang H (2022) Robust PDMS-based porous sponge with enhanced recyclability for selective separation of oil–water mixture. Colloids Surf A Physicochem Eng Asp 648:129228

Wang Y, Wang M, Wang J, Wang H, Men X, Zhang Z (2019) A rapid, facile and practical fabrication of robust PDMS@starch coatings for oil–water separation. J Taiwan Inst Chem Eng 99:215–223

Wang X, Huang L, Zhang C, Deng Y, Xie P, Liu L, Cheng J (2020) Research advances in chemical modifications of starch for

hydrophobicity and its applications: a review. Carbohydr Polym 240:116292

Wang J, Duan H, Wang M, Shentu Q, Xu C, Yang Y, Lv W, Yao Y (2022) Construction of durable superhydrophilic activated carbon fibers based material for highly-efficient oil/water separation and aqueous contaminants degradation. Environ Res 207:112212

Wang X, Cao L, Hu Y, Chen Y, Jin T, Huang J, Zhang X, Lin S (2023) Highly transparent, hydrophobic, hard and flexible coatings based on a novel melamine-formaldehyde resin synthesized by hydrophobic melamine. Prog Org Coat 179:107487

Wen H, Raza S, Wang P, Zhu Z, Zhang J, Huang W, Liang L, Hu H, Deng L, Liu C (2021) Robust super hydrophobic cotton fabrics functionalized with Ag and PDMS for effective antibacterial activity and efficient oil–water separation. J Environ Chem Eng 9:106083

Wu G, Liu D, Chen J, Liu G, Kong Z (2019) Preparation and properties of super hydrophobic films from siloxane-modified two-component waterborne polyurethane and hydrophobic nano SiO_2. Prog Org Coat 127:80–87

Xiong Z, Chen N, Wang Q (2020) Preparation and properties of melamine formaldehyde resin modified by functionalized nano-SiO_2 and polyvinyl alcohol. Polym Polym Compos 29:96–106

Xue J, Yu Y, Bai Y, Wang L, Wu Y (2015) Marine oil-degrading microorganisms and biodegradation process of petroleum hydrocarbon in marine environments: a review. Curr Microbiol 71:220–228

Zhang X, Li Z, Liu K, Jiang L (2013) Bioinspired multifunctional foam with self-cleaning and oil/water separation. Adv Funct Mater 23:2881–2886

Zhang T, Li Z, Lv Y, Liu Y, Yang D, Li Q, Qiu F (2019) Recent progress and future prospects of oil-absorbing materials. Chin J Chem Eng 27:1282–1295

Zhang M, Zhu H, Xi B, Tian Y, Sun X, Zhang H, Wu B (2022) Surface hydrophobic modification of biochar by silane coupling agent KH-570. Processes 10:301

Zhou Q, Liu Q, Song N, Yang J, Ni L (2019) Amphiphilic reactive poly(glycidyl methacrylate)-block-poly(dimethyl siloxane)-block-poly(glycidyl methacrylate) triblock copolymer for the controlling nanodomain morphology of epoxy thermosets. Eur Polym J 120:109236

Zou F, Zhou H, Jeong D, Kwon J, Eom S, Park T, Hong S, Lee J (2017) Wrinkled surface-mediated antibacterial activity of graphene oxide nanosheets. ACS Appl Mater Interfaces 9:1343–1351